

Topological Magnon Insulator in Insulating Ferromagnet

Lifa Zhang,¹ Jie Ren,² Jian-Sheng Wang,¹ and Baowen Li^{1,3,4}

¹*Department of Physics and Centre for Computational Science and Engineering,
National University of Singapore, Singapore 117542, Republic of Singapore*

²*Theoretical Division, Los Alamos National Laboratory, Los Alamos, New Mexico 87545, USA*

³*NUS Graduate School for Integrative Sciences and Engineering, Singapore 117456, Republic of Singapore*

⁴*NUS-Tongji Center for Phononics and Thermal Energy Science and Department of Physics, Tongji University, 200092 Shanghai, PR China*

(Dated: 4 Oct 2012)

In the ferromagnetic insulator with Dzyaloshinskii-Moriya interaction, we theoretically predict and numerically verify a topological magnon insulator, where the charge-free magnon is topologically protected to transport along the edge while it is insulating in the bulk. Within the bulk band gaps, edge states form a connected loop as a 4π - or 8π -period Möbius strip in the wave vector space. As a consequence, the chiral energy current traveling along the corresponding edge is topologically protected from defects or disorders. Using the nonequilibrium Green's function method, we demonstrate that the energy current carried by magnons with energy in the bulk gap localizes at edges and prefers to travel along one edge in only one direction at nonequilibrium steady state. Our prediction about topological magnon insulator could be observed at a wide energy range in the thin film of the insulating ferromagnet, such as $\text{Lu}_2\text{V}_2\text{O}_7$.

PACS numbers: 85.75.-d, 75.30.Ds, 75.47.-m, 75.70.Ak

Topological insulator, as a novel state of quantum matter, is characterized by an insulating bulk band gap and conducting gapless edge/surface states protected by symmetries [1, 2]. It has been theoretically predicted and experimentally observed in a variety of systems and becomes a hot spot because of its theoretical importance in condensed matter physics and wide potential applications in dissipationless spin-based electronics (spintronics) [3]. However, due to the fact that the spin transport in topological insulators is carried by electrons, dissipations can not be really avoided.

Magnon Hall effect, as a consequence of the Dzyaloshinskii-Moriya (DM) interaction [4, 5] which plays a role of vector potential similar to the Lorentz force, has been predicted and observed in magnetic insulators [6–8]. Compared with spin current, where the dissipation from Joule heating is still inevitable due to the electronic carriers, the magnon Hall effect is more promising in device applications because of the long-range coherence of charge-free spin wave [9–11]. Magnons are collective excitations of localized spins in a crystal lattice and can be viewed as quantized quasiparticles of spin waves. Recently, magnon excitation [12, 13], localization [14] and interference [15] have been experimentally realized thanks to the achievements in deposition and nanopatterning techniques. The technical advancements offer the perspective of various magnonic devices, and a new discipline – magnonics – has emerged and growing exponentially [16–19]. The charge-free property of magnon makes it promising to achieve dissipationless transport and control in insulating magnets.

Therefore, it will be of great general interest for both theorists and experimentalists that we find in this work a new intriguing quantum state that magnon while insulated in the bulk, can nondissipatively transport along edges/surfaces in the absence of backscattering from defects and disorders due to the nontrivial topology of magnon's band structures. We

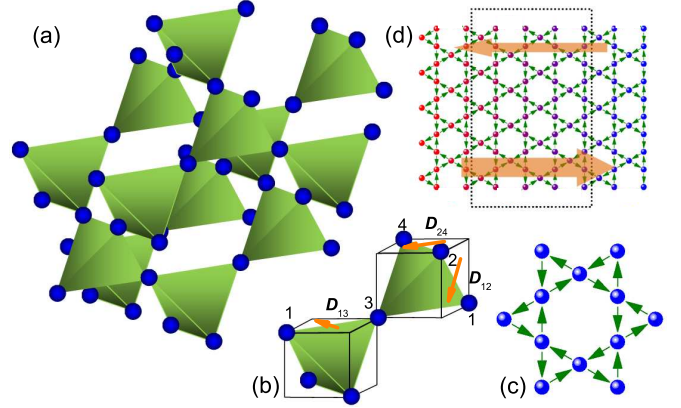


FIG. 1: (color online). (a) Pyrochlore crystallographic structure of the sublattice of magnetic atoms V of $\text{Lu}_2\text{V}_2\text{O}_7$; (b) Two tetrahedrons in the pyrochlore lattice, where DM vectors on bonds 1-3, 1-2, and 2-4 are indicated by orange arrows; (c) Schematic magnetic flux due to DM interaction in the [111] plane of the pyrochlore lattice, i.e., a kagome lattice. The coupling of two sites along the arrows is $(J + iD)S$, and the opposite direction corresponds to $(J - iD)S$; (d) The quasi-one-dimensional strip kagome lattice. The area enclosed by the dotted line can be regarded as a center which is connected to two semi-infinite leads in equilibrium at temperatures T_L (left) and T_R (right). The two big arrows along edges schematically depict the energy flow magnitudes and directions in the lattice when $T_L > T_R$. The width of the strip is $W = 5$, and the number of atoms in each unit cell is $6W - 1$.

name this novel state topological magnon insulator (TMI) and believe that due to the robust dissipationless magnon transport, the TMI in insulating magnets could provide widely potential applications in nondissipative magnonics and microspintronics.

The magnon Hall effect was experimentally observed in insulating ferromagnet $\text{Lu}_2\text{V}_2\text{O}_7$ [7] with a pyrochlore lattice, in which the magnetic atom vanadium has a corner-sharing-

tetrahedra sublattice, that is, a stacking of alternating kagome and triangular lattices along the [111] direction, as shown in Fig. 1 (a). To study magnon transport in the ferromagnetic insulator, the Hamiltonian can be written as [4, 5, 20]:

$$\mathcal{H} = \sum_{\langle mn \rangle} [-J \vec{S}_m \cdot \vec{S}_n + \vec{D}_{mn} \cdot (\vec{S}_m \times \vec{S}_n)] - g\mu_B \vec{H} \cdot \sum_n \vec{S}_n, \quad (1)$$

where \vec{S}_n is the spin angular momentum at site n ; $-J$ denotes the nearest-neighbor coupling; \vec{D}_{mn} is the DM interaction between site m and n ; the last term comes from the Zeeman effect under an external field \vec{H} .

As shown in Fig. 1 (b), in a single tetrahedron, the DM vector is perpendicular to the corresponding bond and parallel to the surface of the surrounding cube [7, 21, 22]. Since the component of \vec{D}_{mn} perpendicular to $\vec{z} = \vec{H}/H$ does not contribute to the Hamiltonian (1) up to quadratic order in $\delta\vec{S}$ [7], we only retain $D_{mn} = \vec{D}_{mn} \cdot \vec{z}$. When applying a magnetic field along $\vec{z} = [111]$ direction, all the projections of the DM interaction between inter-layer sites m and n are zero ($D_{13} = D_{23} = D_{43} = 0$); and all the ones for inner-layer sites are nonzero and equal ($D_{12} = D_{24} = D_{41} \neq 0$). Therefore, with the magnetic field along [111] direction, magnon Hall effect only comes from the noncancellation of different types of loops of DM interaction in the unit cell of the kagome lattice, as shown in Fig. 1 (c). Thus the kagome sublattice structure plays a key role for the presence of magnon Hall effect in $\text{Lu}_2\text{V}_2\text{O}_7$. In the following we first discuss a general kagome lattice with DM interaction; latter we will incorporate actual parameters of a thin film of $\text{Lu}_2\text{V}_2\text{O}_7$ with a kagome layer vanadium sublattice structure.

Using the spin-wave (Holstein-Primakoff) transformation [23, 24], one can straightforwardly obtain the quadratic spin-wave Hamiltonian as [25]:

$$\mathcal{H} = \sum_{mn} b_m^\dagger H_{mn} b_n + E_0, \quad (2)$$

where b^\dagger/b denotes the operator that increases/decreases the spin component along $\vec{z} = [111]$ which is also the direction of the applied magnetic field, $H_{mn} = H_{nm}^* = (J \pm iD)S$, $m \neq n$, $H_{mm} = JSM_n + hS$, M_n is the number of nearest neighbors of site n . The ground-state energy reads $E_0 = -JS^2 \sum_n M_n/2 - NhS$ with N the total number of sites and $h = g\mu_B H$. We set $D_{mn} = D$ and the kagome lattice with DM interaction is shown in Fig. 1 (c), where the coupling between two sites along the direction of that arrow corresponds to $(J + iD)S$, and the opposite direction corresponds to $(J - iD)S$ [25]. Due to the different types of loops in a unit cell of the kagome lattice, the DM interaction avoids cancellation thus induces the Hall effect [6]. As a consequence, the DM interaction acts as a vector potential for the propagation of magnons similar to the magnetic field for the propagation of electrons. In the following calculations, we use dimensionless units and set $S = 1/2$, and $J = 1$ without loss of generality. The magnetic field decides the direction of spins at the ground state, and the induced Zeeman effect term

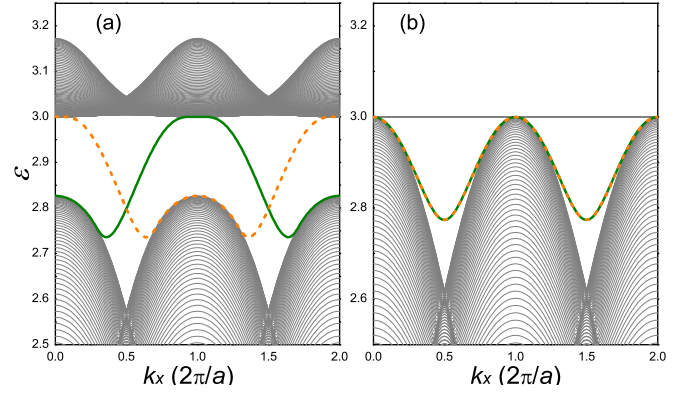


FIG. 2: (color online). The upper part of the dispersion relation of kagome lattice strip in the range of $k_x = 0 \sim 4\pi/a$ (a is the lattice constant), with (a) $D/J = 0.1$, and (b) zero DM interaction.

shifts the dispersion relation. We set magnetic field $H = 0^+$ in the first part of theoretical calculations, and will input finite H in the later part for real-material calculations.

With the bosonized Hamiltonian (2), we are able to calculate the magnon's band structure as well as the Berry curvature and Chern number for each band [26]. To investigate the edge magnon transport, we carry out the calculation and analysis based on the strips of two-dimensional kagome lattice structure as shown in Fig. 1 (d). The dispersion relation of magnons (ε vs k_x) in the infinitely long strip with DM interaction is displayed in Fig. 2 (a). Since there are three sites in each kagome unit cell, there are three energy bands separated by two energy gaps. With increasing strip width, more modes appear in the energy bands; the edge states will be gradually fixed and independent of size [27]. When the system width is finite, the states in two edges could couple together to open an energy gap, which exponentially decays with width increasing [25, 28]. When the strip width increases to infinity, the edges are separated too far to interact with each other; thus they could have degeneracy in dispersions, as shown in Fig. 2. In our calculation, the edge states are almost invariable when the width $W \geq 20$ [25] and we use width $W = 80$ in all the latter numerical calculations. Because of the DM interaction, two edge states within both energy gaps are twisted so that for each state $\varepsilon(\pi/a - k_x) \neq \varepsilon(\pi/a + k_x)$, and they cross at $k_x = \pi/a$ in the first Brillouin zone, as shown in Fig. 2 (a). As a consequence, the two edge modes form a continuous state with a period of 4π , which can not be disturbed to open a gap by weak disorders so that edge modes are topologically protected. However, when DM interaction is zero, the two edge states are easy to be perturbed to separate and open a gap, because they do not cross with each other although they degenerate as shown in Fig. 2 (b).

In the lower bulk band gap, we find that four edge states will contribute to magnon transport within the energy gap, as shown in Fig. 3 (a). If $D/J \approx 0.4$ or larger, in both energy gaps there are four edge states. In a period of 8π , any two of the four edge states have degeneracies and cross each other

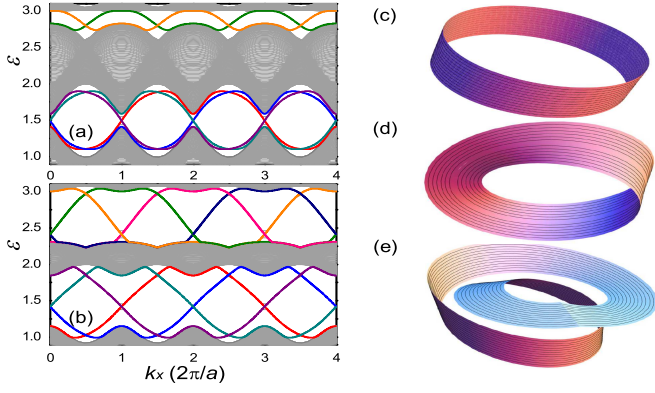


FIG. 3: (color online). The dispersion relation of edge modes with non-zero DM interactions. (a) and (b) are dispersion relations in range of $k_x = 0 \sim 8\pi/a$ for $D/J = 0.1$ and 0.4 , respectively. (c) A conventional cylinder strip with two boundaries, of which each has a period of 2π ; (d) A Möbius strip which only has one boundary of 4π period; (e) A looped Möbius strip which only has one boundary of 8π period.

at different points in the momentum space. All the four edge states form a continuous state with a period of 8π to transport magnons along two edges of the strip. We can understand the topology of the edge states as follows. With zero DM interaction, the edge states are similar to the two boundaries of the conventional cylindric strip as shown in Fig. 3 (c), both of which have a period of 2π in Brillouin zone and transport separately along two edges. Due to the nonzero DM interaction, two edge states are twisted so that they cross each other and go into the other energy band after 2π in momentum space, thus form a closed loop with a period of 4π . These edge states are similar to the one-sided Möbius strip with only one boundary, as shown in Fig. 3 (d), where a line drawn starting from a point at the boundary will meet back at the “other side” after a circle of 2π , then go back to the original point after a whole period of 4π . The two edge states form one closed loop winding the bulk energy gap between the two bands, which are thus topologically protected from distortions. At larger DM interaction, four edge states contribute to the transport in the bulk gap, cross each other, and connect to form a closed 8π -period loop which can be interpreted as the only one boundary of a looped Möbius strip as shown in Fig. 3 (e). This looped Möbius strip also has only one boundary winding around the strip surface, thereby having the same topology as that of the conventional Möbius strip shown in Fig. 3 (d).

The edge state transport is related to the band topology characterized by Chern numbers of the bulk states [27, 29–31]. When the DM interaction is absent, all the Chern numbers of three bands are zero so that there is no magnon Hall effect [25]. Accordingly, the winding numbers of edge states are zero as well, thus they are not topologically protected. With nonzero DM interaction, the Chern numbers of the lowest and highest energy bands become ± 1 ; the one of the middle energy band is still zero [25]. According to the relation between the Chern number and the winding number [27], the winding

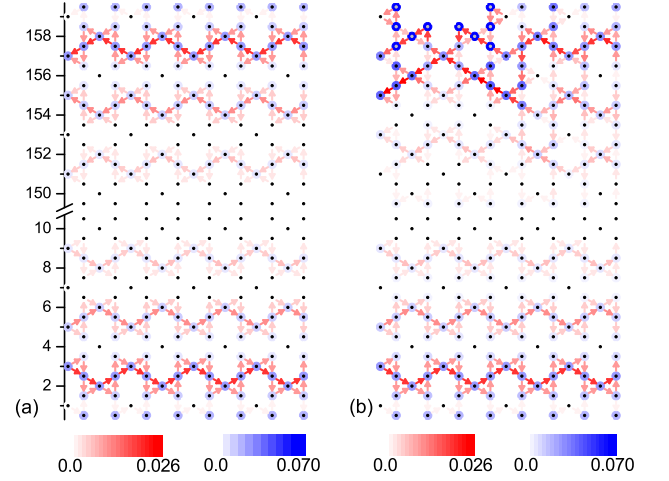


FIG. 4: (color online). The local energy current and density of state for edge magnon transport at equilibrium. (a) The uniform kagome lattice. (b) The lattice with a defect at the upmost site of the left fifth column. The red arrows, the blue dots, and the small black dots correspond to the local energy current, the local density of magnon, and atom sites, respectively. The color of the arrow indicates the magnitude of the local current. Parameters are $\varepsilon = 1.5$, $T_L = T_R = 1.0$, $D/J = 0.1$, lattice spacing $a = 1$.

numbers of edge states in both bulk gaps have the same value of 1 or -1 , which is consistent with the only one closed loop winding the bulk gap regardless of the period of 4π , 8π or others.

To intuitively illustrate the magnon transport by edge states, we choose some unit cells of the kagome lattice strip as a center region and set the rest two semi-infinite lattices in equilibrium at temperatures T_L and T_R to study the energy transport by magnons as shown in Fig. 1 (d). Fig. 4 shows the edge state magnon transport in the bulk gap at a fixed magnon energy $\varepsilon = 1.5$ in thermal equilibrium. The forward (left-to-right) thermal current carried by magnons travels along one edge, and the backward (right-to-left) current with the same magnitude transports along the other one, as shown in Fig. 4 (a). Near both edges the local magnon currents form many chiral vortices due to the nonzero DM interaction. Moreover, both the current and the magnon density of states are symmetrically localized at two edges. They exponentially decay from the edge to the center with oscillations [25], which is similar to the properties of the localized edge phonon modes [32] and electron transport in graphene [33]. If the DM interaction reverses ($D \rightarrow -D$), all the currents reverse to the opposite direction.

When a defect is present at one edge, the current take a detour around it and transports ahead without backscattering, as illustrated in Fig. 4 (b). Although the defect dramatically affects the local density of magnons and destroys the local current vortex, the global currents along two edges keep intact compared to those of the uniform lattice, and their summation keeps zero since the net transport vanishes at equilibrium.

For the nonequilibrium case that two leads are held at dif-

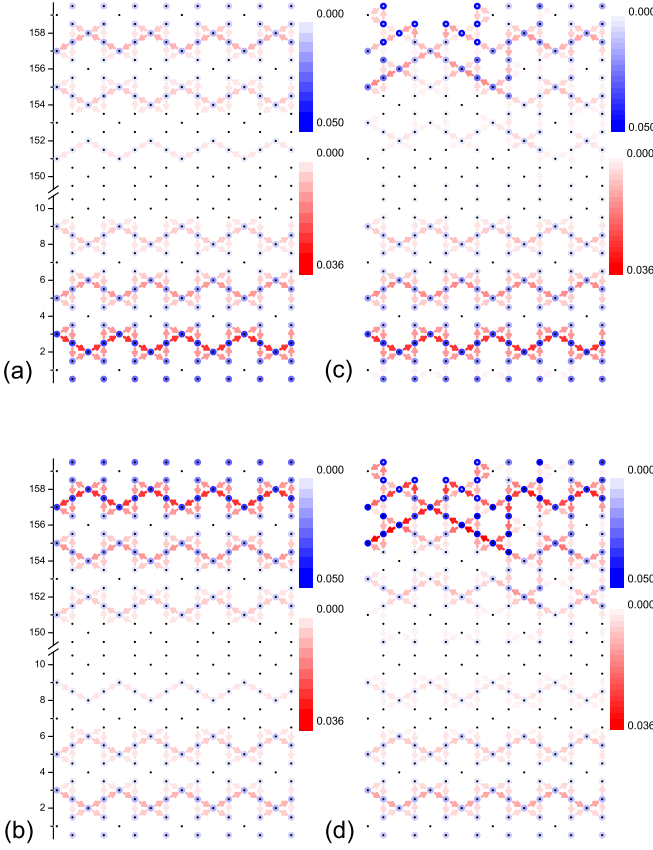


FIG. 5: (color online). The local energy current and density of state for edge magnon transport at nonequilibrium. The uniform kagome lattice are with (a) $T_L = 1.2, T_R = 0.8$, and (b) $T_L = 0.8, T_R = 1.2$. The lattice with a defect at the upmost site of the left fifth column are with (c) $T_L = 1.2, T_R = 0.8$, and (d) $T_L = 0.8, T_R = 1.2$. Other parameters are $\varepsilon = 1.5$, $D/J = 0.1$, $a = 1$, $W = 80$.

ferent temperatures, the magnon will prefer to flow along one edge in the steady state, see Fig. 5 (a) and (b). For positive DM interaction and $T_L > T_R$, the forward thermal current transported along the lower edge is larger than the backward one along the upper edge. The summation of forward and backward currents along two corresponding edges satisfies the Landauer formula. If we swap the temperatures of the left and right end, the thermal current will prefer the other edge. If the defect is present, both the local density of magnon and the local thermal current will be affected. However, the one-way edge magnon transport can detour the defect and keep the same magnitude to flow ahead, see Fig. 5 (c) and (d). In this way, the global thermal current keeps invariant, which means that the edge state in the bulk gap is indeed topologically protected from the lattice defect or disorder.

With the help of nonzero DM interactions, the magnon chirally travels along the corresponding edge nondissipatively in the absence of backscattering, which is preserved from weak defects or disorders. We use the actual parameters of thin film of $\text{Lu}_2\text{V}_2\text{O}_7$, to investigate the energy range of magnons for observing the TMI. As shown in Fig. 6 (a), the energy cur-

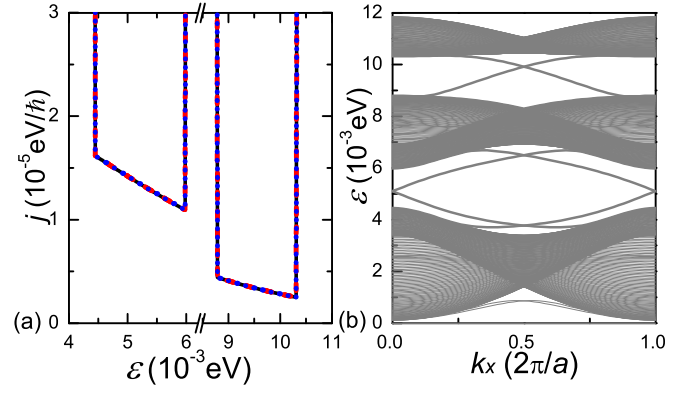


FIG. 6: (color online). The current density vs energy of magnon for uniform and edge-defect kagome lattices with the parameters of $\text{Lu}_2\text{V}_2\text{O}_7$. (a) The solid and dotted lines correspond to the thermal current in the bulk band gaps for uniform and edge-defect lattices, respectively. (b) The dispersion relation of the kagome lattice with the parameters of $\text{Lu}_2\text{V}_2\text{O}_7$. $D/J = -0.26$, $H = 1$ T, $T_L = 21$ K, and $T_R = 19$ K.

rent of magnon is not affected by defect or disorder in the energy range of $[4.45, 5.98] \cup [8.79, 10.31]$ meV. These energy ranges coincide with the bulk gaps in the energy spectrum where the topological magnon edge states can be found [see Fig. 6 (b)]. Although certain distortions of edge states will occur as results of the defect or disorder, the energy current carried by magnons has no difference in the whole bulk energy gap. This indicates that the defect or disorder does not open a gap in the energy spectrum so that the topology of the magnon edge state is robust. According to the energy ranges, the topological magnons have frequencies ranging from $[1.08, 1.45] \cup [2.13, 2.49]$ THz. Applying different external magnetic fields will not change the main properties of magnons, but shift the corresponding dispersion relations [25], so that the frequency of topological magnons can be tuned flexibly with a wide range. Therefore, we expect that for the thin film of $\text{Lu}_2\text{V}_2\text{O}_7$ in a wide energy range of magnons, one can observe the TMI, which could also be highly likely for other magnetic insulators containing the kagome lattice structure.

To realize magnonic devices as well as the predicted TMI, the excitation and detection of magnons is the major challenge. Recent years have witnessed a fast development in experimental techniques such as ferromagnetic resonance [15], pulse-inductive microwave magnetometer [34], time-resolved scanning Kerr microscopy [35], optical pump-probe techniques [36], as well as Brillouin light scattering (BLS) [37] which takes a special role since it allows the direct measure of dispersions and band structures. We could observe the topological edge modes by using these techniques to measure the magnon dispersion relation and could also verify the TMI by detecting the magnon transport in the bulk band gap where magnons could be excited by non-thermal optical pulses [38] or spin-polarized current [39], so that we can avoid the thermal transport due to the bulk states thus extract only the edge

channels. We hope our theoretical predictions about TMI could open a new window into the application of nondissipative magnon transport, especially for the novel magnonic device design, which could also shed light on the information technology based on magnonics, and micro-spintronics.

L. Z. and B. L. are supported by the grant R-144-000-285-646 from Ministry of Education of Republic of Singapore. J. R. acknowledges the support of the U.S. Department of Energy through the LANL/LDRD Program. J.-S. W. acknowledges support from a URC research grant R-144-000-257-112 of NUS.

-
- [1] M. Z. Hasan, and C. L. Kane, *Rev. Mod. Phys.* **82**, 3045 (2010).
 - [2] X.-L. Qi, and S.-C. Zhang, *Rev. Mod. Phys.* **83**, 1057 (2011).
 - [3] I. Žutić, J. Fabian, and S. Das Sarma, *Rev. Mod. Phys.* **76**, 323 (2004).
 - [4] I. Dzyaloshinskii, *J. Phys. Chem. Solids* **4** 241 (1958).
 - [5] T. Moriya, *Phys. Rev.* **120**, 91 (1960).
 - [6] H. Katsura, N. Nagaosa and P. A. Lee, *Phys. Rev. Lett.* **104**, 066403 (2010).
 - [7] Y. Onose, T. Ideue, H. Katsura, Y. Shiomi, N. Nagaosa, and Y. Tokura, *Science* **329**, 297 (2010).
 - [8] R. Matsumoto and S. Murakami, *Phys. Rev. Lett.* **106**, 197202 (2011).
 - [9] J. E. Hirsch, *Phys. Rev. Lett.* **83**, 1834 (1999).
 - [10] S. Murakami, N. Nagaosa, and S.-C. Zhang, *Science* **301**, 1348 (2003).
 - [11] J. Sinova, D. Culcer, Q. Niu, N. A. Sinitsyn, T. Jungwirth, and A. H. MacDonald, *Phys. Rev. Lett.* **92**, 126603 (2004).
 - [12] A. A. Serga, S. O. Demokritov, B. Hillebrands, and A. N. Slavin, *Phys. Rev. Lett.* **92**, 117203 (2004).
 - [13] V. E. Demidov, M. P. Kostylev, K. Rott, P. Krzysteczko, G. Reiss, and S. O. Demokritov, *Appl. Phys. Lett.* **95**, 112509 (2009).
 - [14] J. Jorzick, S. O. Demokritov, B. Hillebrands, M. Bailleul, C. Fermon, K. Y. Guslienko, A. N. Slavin, D. V. Berkov, and N. L. Gorn, *Phys. Rev. Lett.* **88**, 047204 (2002).
 - [15] J. Podbielski, F. Giesen, and D. Grundler, *Phys. Rev. Lett.* **96**, 167207 (2006).
 - [16] V. V. Kruglyak, and J. Hicken, *Magn. Magn. Mater.* **306**, 191 (2006).
 - [17] S. Neusser, and D. Grundler, *Adv. Mater.* **21**, 2927 (2009).
 - [18] A. A. Serga, A. V. Chumak, and B. J. Hillebrands, *Phys. D: Appl. Phys.* **43**, 264002 (2010).
 - [19] B. Lenk, H. Ulrichs, F. Garbs, M. Münzenberg, *Physics Reports* **507**, 107 (2011).
 - [20] I. Bose, and U. Bhaumik, *J. Phys.: Condens. Matter* **6** 10617 (1994).
 - [21] M. Elhajal, B. Canals, R. Sunyer, and C. Lacroix, *Phys. Rev. B* **71**, 094420 (2005).
 - [22] V. N. Kotov, M. Elhajal, M. E. Zhitomirsky, and F. Mila, *Phys. Rev. B* **72**, 014421 (2005).
 - [23] T. Holstein and H. Primakoff, *Phys. Rev.* **58**, 1098(1940).
 - [24] L. Zhang, J.-S. Wang, and B. Li, *Phys. Rev. B* **78**, 144416 (2008).
 - [25] See the detailed discussion in supplementary information.
 - [26] L. Zhang, J. Ren, J.-S. Wang, and B. Li, *Phys. Rev. Lett.* **105**, 225901 (2010); *J. Phys.: Condens. Matter* **23**, 305402 (2011).
 - [27] Y. Hatsugai, *Phys. Rev. B* **48**, 11851 (1993); *Phys. Rev. Lett.* **71**, 3697 (1993).
 - [28] B. Zhou, H.-Z. Lu, R.-L. Chu, S.-Q. Shen, and Q. Niu, *Phys. Rev. Lett.* **101**, 246807 (2008).
 - [29] X.-L. Qi, Y.-S. Wu, and S.-C. Zhang, *Phys. Rev. B* **74**, 045125 (2006).
 - [30] V. W. Scarola, and S. D. Sarma, *Phys. Rev. Lett.* **98**, 210403 (2007).
 - [31] W. Yao, S. A. Yang, and Q. Niu, *Phys. Rev. Lett.* **102**, 096801 (2009).
 - [32] J.-W. Jiang, J. Chen, J.-S. Wang, and B. Li, *Phys. Rev. B* **80**, 052301 (2009).
 - [33] Z. Qiao, S. A. Yang, W. Feng, W.-K. Tse, J. Ding, Y. Yao, J. Wang, and Q. Niu, *Phys. Rev. B* **82**, 161414(R) (2010).
 - [34] T. J. Silva, C. S. Lee, T. M. Crawford, and C. T. Rogers, *J. Appl. Phys.* **85**, 7849(1999).
 - [35] A. Barman, V. V. Kruglyak, R. J. Hicken, A. Kundrotaite, and M. Rahman, *Appl. Phys. Lett.* **82**, 3065 (2003).
 - [36] A. V. Kimel, A. Kirilyuk, F. Hansteen, R. V. Pisarev, and T. Rasing, *J. Phys.: Condens. Matter* **19**, 043201 (2007).
 - [37] K. Perzlmaier, M. Buess, C. H. Back, V. E. Demidov, B. Hillebrands, and S. O. Demokritov, *Phys. Rev. Lett.* **94**, 57202 (2005).
 - [38] A. V. Kimel, A. Kirilyuk, A. Tsvetkov, R. V. Pisarev, and T. Rasing, *Nature* **429**, 850 (2004).
 - [39] S. I. Kiselev, J. C. Sankey, I. N. Krivorotov, N. C. Emley, R. J. Schoelkopf, R. A. Buhrman, and D. C. Ralph, *Nature* **425**, 380 (2003).